the plant journal

SEB Society for Experimental Biology

The Plant Journal (2015) **84,** 773–784 doi: 10.1111/tpj.13038

SCARECROW-LIKE23 and SCARECROW jointly specify endodermal cell fate but distinctly control SHORT-ROOT movement

Yuchen Long[1,2,†], Joachim Goedhart[3], Martinus Schneijderberg[2], Inez Terpstra[2], Akie Shimotohno[2], Benjamin P. Bouchet[4], Anna Akhmanova[4], Theodorus W. J. Gadella Jr[3], Renze Heidstra[1,2], Ben Scheres[1,2] and Ikram Blilou[1,2,*]

[1]*Plant Developmental Biology, Plant Sciences, Wageningen University and Research Centre, Droevendaalsesteeg 1, Wageningen 6708PB, the Netherlands,*

[2]*Molecular Genetics, Department Biology, Padualaan 8, Utrecht 3581CH, the Netherlands,*

[3]*Swammerdam Institute for Life Sciences, Section of Molecular Cytology, van Leeuwenhoek Centre for Advanced Microscopy, University of Amsterdam, Science Park 904, Amsterdam 1098 XH, the Netherlands, and*

[4]*Cell Biology, Department Biology, Utrecht University, Padualaan 8, Utrecht 3581CH, the Netherlands*

Received 3 July 2015; revised 15 September 2015; accepted 18 September 2015; published online 28 September 2015.

*For correspondence (e-mail Ikram.blilou@wur.nl).

[†]Present address: Laboratoire de Reproduction et Développement des Plantes, INRA, CNRS, ENS, UCB Lyon 1, 46 Allée d'Italie, 69364, Lyon Cedex 07, France.

SUMMARY

Intercellular signaling through trafficking of regulatory proteins is a widespread phenomenon in plants and can deliver positional information for the determination of cell fate. In the *Arabidopsis* root meristem, the cell fate determinant SHORT-ROOT (SHR), a GRAS domain transcription factor, acts as a signaling molecule from the stele to the adjacent layer to specify endodermal cell fate. Upon exiting the stele, SHR activates another GRAS domain transcription factor, SCARCROW (SCR), which, together with several BIRD/INDETERMINATE DOMAIN proteins, restricts movement of SHR to define a single cell layer of endodermis. Here we report that endodermal cell fate also requires the joint activity of both SCR and its closest homologue SCARECROW-LIKE23 (SCL23). We show that SCL23 protein moves with zonation-dependent directionality. Within the meristem, SCL23 exhibits short-ranged movement from ground tissue to vasculature. Away from the meristem, SCL23 displays long-range rootward movement into meristematic vasculature and a bidirectional radial spread, respectively. As a known target of SHR and SCR, SCL23 also interacts with SCR and SHR and can restrict intercellular outspread of SHR without relying on nuclear retention as SCR does. Collectively, our data show that SCL23 is a mobile protein that controls movement of SHR and acts redundantly with SCR to specify endodermal fate in the root meristem.

Keywords: endodermal fate, mobile protein, SCL23, intercellular movement, protein interaction, SCR–SHR complex, *Arabidopsis thaliana*.

INTRODUCTION

In plants, cell–cell trafficking of regulatory proteins is widely used for intercellular communication during specification of cell fate (Sparks *et al.*, 2013). In this context, mobile transcription factors can convey positional information in a non-cell-autonomous manner (Scheres, 2001; Dolan, 2006; Gallagher *et al.*, 2014; Han *et al.*, 2014; Long *et al.*, 2015a).

The maize homeodomain protein KNOTTED1 (KN1) was the first mobile transcription factor to be described in plants. Loss-of-function *knotted* mutants failed to form a shoot meristem, while gain-of-function mutants produced ectopic knots (Schneeberger *et al.*, 1995; Kerstetter *et al.*, 1997). Both KN1 protein and its mRNA can traffic within the shoot meristem and across tissue layers in the leaf (Lucas *et al.*, 1995; Kim *et al.*, 2002). In addition, KN1 was shown to potentiate its own transport between cells by interacting with plasmodesmata (PD) intercellular membrane-bound channels, and increasing its size-exclusion limit (Lucas *et al.*, 1995; Kragler *et al.*, 2000). Mobility of KN1, which requires its homeodomain region, was shown to be necessary to rescue mutant phenotypes (Kim *et al.*, 2002, 2005). In *Arabidopsis*, SHOOTMERISTEMLESS (STM)

and KNAT1 are KN1 orthologs (Long *et al.*, 1996; Reiser *et al.*, 2000; Vollbrecht *et al.*, 2000) that contain the conserved homeodomain to confer their intercellular mobility within the shoot apical meristem, leaves and stem (Kim *et al.*, 2003). Movement of KNAT1 was shown to be required for epidermal cell differentiation, indicating the significance of its mobility during development (Rim *et al.*, 2009).

LEAFY (LFY) was also shown to move between cells in the *Arabidopsis* flower meristem (Sessions *et al.*, 2000), where it is required for triggering expression of floral identity genes (Weigel *et al.*, 1992; Lohmann *et al.*, 2001). Unlike KN1, LFY exhibits a movement pattern that resembles diffusion (Wu *et al.*, 2003).

Since the discovery of KN1 and LFY, many mobile transcription factors have been described (Rim *et al.*, 2011; Han *et al.*, 2014; Mähönen *et al.*, 2014). However, among all the characterized mobile transcription factors, the GRAS domain protein SHORT-ROOT (SHR) remains the best-studied example in which its movement is related to specification of cell fate in the root meristem (Nakajima *et al.*, 2001; Sena *et al.*, 2004; Cui *et al.*, 2007; Cruz-Ramírez *et al.*, 2012; Long *et al.*, 2015b). SHR traffics from the stele to the surrounding cell layer where it binds to its target SCARECROW (SCR), another GRAS domain transcription factor, and acts as a SHR–SCR complex to specify the quiescent center (QC) and promote asymmetric cell division of the cortex/endodermis initial (CEI) (Nakajima *et al.*, 2001; Sabatini *et al.*, 2003; Heidstra *et al.*, 2004; Cruz-Ramírez *et al.*, 2012, 2013). In addition, regulation of radial SHR distribution is essential for specifying endodermal cell fate and stabilizing tissue boundaries in the root meristem; movement of SHR is restricted through a nuclear retention mechanism by binding to SCR and several BIRD/INDETERMINATE DOMAIN proteins such as JACKDAW (JKD) and BALDIBIS (BIB) (Long *et al.*, 2015b). SHR activates *SCR* to trigger its own nuclear confinement in the endodermis (Levesque *et al.*, 2006; Cui *et al.*, 2007), and together with JKD and BIB acting upstream of *SCR*, they form a positive feedback loop which fortifies nuclear accumulation of SHR to prevent its outward spread (Long *et al.*, 2015b).

Here we present an analysis of SCARECROW-LIKE23 (SCL23), another GRAS domain protein closely related to SCR and recently identified as a common target of SCR and SHR (Cui *et al.*, 2014). We show that SCL23 is a mobile protein that acts redundantly with SCR to regulate endodermal fate in the root meristem. We show that in the meristem SCL23 exhibits short-range mobility from the ground tissue to the stele, while in the transition and elongation zones SCL23 displays long-range rootward movement into the meristem with a capacity for bidirectional radial spreading. We also show that SCL23 restricts outward movement of SHR through a mechanism that does not involve nuclear retention. Furthermore, we demonstrate that SCL23 and SCR antagonistically regulate each other's expression, while their collective activity is required to specify endodermal cell fate.

RESULTS

SCL23 interacts with SHR and SCR *in vivo*

The SCR and SHR proteins form a complex required for controlling asymmetric cell division in the cortex–endodermis initial and its daughter (CEI/D) within the *Arabidopsis* root (Cruz-Ramírez *et al.*, 2012). A genetic screen for factors controlling this division identified JKD, a member of the BIRD family, as a factor involved in this process. JACKDAW was shown to form protein complexes with both SCR and SHR (Welch *et al.*, 2007; Long *et al.*, 2015b). SHORT-ROOT is required for the specification of endodermal fate (Helariutta *et al.*, 2000) through the collective activities of subsets of BIRD proteins and SCR (Long *et al.*, 2015b). As BIRD proteins on their own were not competent to confer endodermal fate (Long *et al.*, 2015b), we hypothesized that a complex involving SHR and SCR may be decisive in instructing endodermal fate.

To identify a potential partner with a redundant role in this process we performed a yeast two-hybrid screen with SCR as bait and selected for candidates with enriched expression in the ground tissue (Birnbaum *et al.*, 2005; Brady *et al.*, 2007) and isolated SCL23, the closest homolog to SCR in *Arabidopsis* (Lee *et al.*, 2008).

We verified the *in vivo* interaction of SCR and SCL23 by performing a bimolecular fluorescence complementation (BiFC) assay in *Arabidopsis* mesophyll protoplasts (Figure 1b,c; Lee *et al.*, 2008). Interestingly, SCL23 could also bind SHR, and the resulting complex was observed in both the nuclei and cytoplasm of the protoplasts (Figure 1c), while SCL23 interacted with SCR predominantly in the nuclei (Figure 1a,b). We further confirmed the interaction between SCL23 and SHR by the Förster resonance energy transfer measurement using fluorescence-lifetime imaging microscopy (FRET-FLIM) approach in protoplasts and HeLa cells (Figures 1e and S1). The FRET measurements indicated that SCL23 had comparable binding capacity to SHR as to SCR (Figure 1e), and the SCL23–SHR complex had the same level of interaction in the nuclei and cytoplasm in HeLa cells, signified by the homogeneous lifetime heat map and the single peak in the lifetime histogram (Figure S1c). Thus, different approaches reveal that SCL23 binds to SCR and SHR, and that the SHR–SCL23 interaction is observed in both the nuclei and cytoplasm.

The SCR and SCL23 proteins act redundantly to specify endodermal fate

Mutations in *SCR* result in roots with a single ground tissue layer exhibiting mixed characteristics of cortex and endodermis (Benfey *et al.*, 1993; Di Laurenzio *et al.*, 1996).

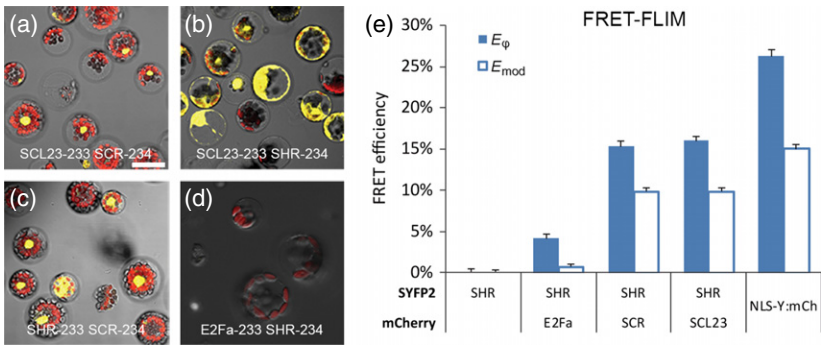

Figure 1. SCARECROW-LIKE23 (SCL23) binds to SCARECROW (SCR) and SHORT-ROOT (SHR).
(a)–(d) Bimolecular fluorescence complementation assay in *Arabidopsis* mesophyll protoplasts showing interactions between SCL23 and SHR or SHR. E2Fa-SHR was used as a negative control, while SHR–SCR was used as a positive control (Cruz-Ramírez *et al.*, 2012). Note the nucleocytoplasmic interaction signal between SCL23 and SHR. Scale bar = 20 μm.
(e) Frequency-domain Förster resonance energy transfer measurement using the fluorescence-lifetime imaging microscopy (FRET-FLIM) analysis of *Arabidopsis* mesophyll protoplasts showing interactions between SCR, SCL23 and SHR. Error bars indicate standard errors of means. E2Fa-SHR was used as a negative control, while a nuclear-localizing YFP:mCherry tandem was used as a positive control (Long *et al.*, 2015b). E_φ, FRET efficiency derived from fluorescence phase-shift information; E_{mod}, FRET efficiency derived from fluorescence demodulation.

The SCL23 protein displayed close homology to SCR; in addition, SCL23 interacted physically with both SCR and SHR. To assess functional redundancy between these two close homologs, we generated a *scr scl23* double mutant. Single mutants of *scl23* have been reported to have no obvious developmental phenotypes (Lee *et al.*, 2008; Cui *et al.*, 2014). However, root growth and the meristem size of *scr scl23* seedlings resembled the *shr* phenotype (Figure 2a–c,d–h). We analyzed the *scr scl23* ground tissue monolayer for endodermal features using autofluorescence of Casparian strips as a key morphological mark for endodermis. The *scl23* single mutant, similar to the wild type (WT), displayed Casparian strip marks in its designated endodermal layer (Figure 2e′). In *scr* mutant roots, as previously shown, the ground tissue monolayer retained Casparian strips (Figure 2f′; Di Laurenzio et al., 1996). However, in *scr scl23* roots, the mutant monolayer did not show any Casparian strips, similar to *shr* (Figure 2g′,h′; Helariutta *et al.*, 2000). These data indicate that the *scr scl23* double mutant contains no endodermal tissue and superficially mimics *shr* in root development.

We next examined the *scl23 shr* phenotype and found it to be similar to *shr* (Figure 2i,i′).

The SCL23 protein shows stele enrichment in the root meristem

To determine the expression domain of *SCL23*, we generated *pSCL23::NLS-3YFP* and *pSCL23::SCL23:YFP* reporter constructs, and transformed them into WT *Arabidopsis*. Analysis of promoter activity indicated that the *SCL23* transcription domain resides predominantly in the mature endodermis and cortex of *Arabidopsis* roots, starting from the transition zone shootwards, which largely represented the published microarray data (Figure 3a; Birnbaum *et al.*, 2005; Brady *et al.*, 2007). In the meristem, *pSCL23::NLS-3YFP* signal could be detected occasionally in the ground tissue cells adjacent to the stem cell niche (Figure 3a). The SCL23:YFP protein fluorescent signal, however, was observed not only in the ground tissue but also in the stele where no *SCL23* promoter activity was detected (Figure 3b). We found SCL23:YFP localized to both the nuclei and cytoplasm of root cells, similar to SHR (Figure 3b). Such a subcellular localization of SCL23, together with its presence in the stele, is consistent with the observed nucleocytoplasmic interaction of SCL23–SHR in protoplast cells (Figure 1b).

The SCL23 protein can restrict exit of SHR from the stele

Given the interaction between SCL23 and SHR, the close homology between SCL23 and SCR and the role of SCR in restricting movement of SHR, we hypothesized that SCL23 might also constrain movement of SHR. As ectopic SCR expression in the stele abolished outward movement of SHR by promoting its nuclear retention (Figure 4c; Koizumi *et al.*, 2012; Long *et al.*, 2015b), we assessed the significance of the vascular meristematic accumulation of SCL23 protein by increasing its levels in vasculature using the *WOODENLEG* promoter (*pWOL*; Bonke *et al.*, 2003). We noticed that in roots expressing *pWOL::SCL23,* the endodermis and cortex failed to completely separate, resulting in patches of ground tissue monolayer in the root meristem (Figure 4b). This phenotype was reminiscent of ectopic expression of SCR in the stele. We next monitored movement of SHR by introducing *pWOL::SCL23* into *pSHR::SHR:YFP* plants, and found that SHR:YFP could not be detected in the monolayer (Figure 4b). These data indicate that SCL23 is able to constrain intercellular movement of SHR.

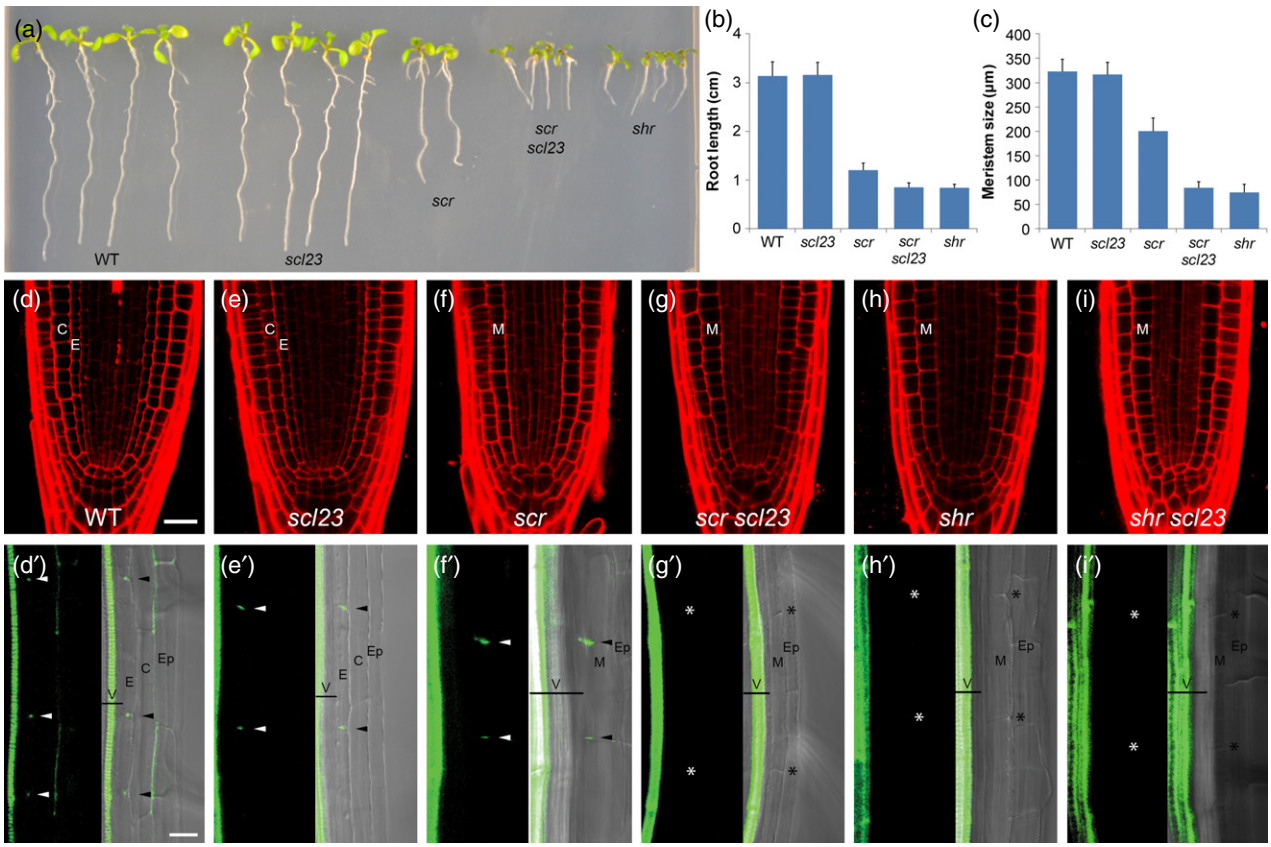

Figure 2. SCARECROW-LIKE23 (SCL23) and SCARECROW (SCR) are required for specification of endodermal fate.
(a) Root length of seedlings of wild type (WT), *scl23*, *scr*, *scr scl23* and *shr* 5 days post-germination (dpg). (b) Root length quantifications of the genotypes in (a) at 5 dpg. Error bars represent standard errors of means: WT $n = 21$, *scr* $n = 19$, *scr scl23* $n = 22$, *shr* $n = 22$. (c) Meristem cell number determined by cortex cells of the genotypes in (a) at 4 dpg. Error bars represent standard errors of means: WT $n = 12$, *scr* $n = 13$, *scr scl23* $n = 14$, *shr* $n = 13$. (d)–(i) Root meristems of 3-dpg WT (d), *scl23* (e), *scr* (f), *scr scl23* (g), *shr* (h) and *shr scl23* (i). (d′)–(i′) Casparian strip staining in the genotypes in (d). The left panel shows the fluorescent signal of Casparian strips and xylems, while the right panel shows such signals overlaid with the light transmission image. Arrowheads point to Casparian strips. Asterisks mark the positions of ground tissue cell walls without Casparian strip staining. V, vasculature; E, endodermis; C, cortex; Ep, epidermis; M, ground tissue monolayer. Scale bars = 20 μm unless specifically indicated in the figure.

Previously, SCR had been described to restrict movement of SHR by a mechanism that involves nuclear retention through the formation of a protein complex (Figure 4c; Cui *et al.*, 2007; Long *et al.*, 2015b). We asked whether SCL23 acts similarly to SCR by retaining SHR in the nucleus. Analysis of *pSHR::SHR:YFP* roots with ectopic *pWOL::SCL23* expression revealed that SHR:YFP maintained its dual nucleocytoplasmic localization (Figure 4b). We also introduced SHR, SCR and SCL23 into a heterologous system of HeLa cells to prevent interference from plant-specific factors, and verified that SCL23 did not confer nuclear enrichment in SHR as SCR did (Figure 4d–h).

Formative divisions in the ground tissue are controlled by SCL23 and SCR through mutual repression

Endodermal SHR activates *SCR* to promote the formative divisions that separate cortex and endodermis (Nakajima *et al.*, 2001; Cruz-Ramírez *et al.*, 2012). Since *pWOL::SCL23* blocked exit of SHR from the stele, we asked whether retention of SHR resulted in reduced levels of SCR, preventing formative divisions. We monitored *pSCR::SCR:CFP* expression in *pWOL::SCL23* lines and found that, consistent with retarded movement of SHR, accumulation of SCR:CFP was undetectable in the meristem (Figure 5a,b′). In the transition zone where *pWOL::SCL23:YFP* level was reduced, SCR:CFP reappeared and both ground tissue layers could be detected (Figure 5b,b′). These data suggest that high levels of SCL23 can control formative divisions in the ground tissue by regulating the range of action of SHR.

SHORT-ROOT and SCR are described to share a common set of transcriptional targets, including *SCR* itself and *SCL23* (Levesque *et al.*, 2006; Cui *et al.*, 2007, 2014). We determined whether *SCL23* is transcriptionally dependent on SCR and/or SHR by quantitative (q)RT-PCR and found a reduced expression in *shr* mutant roots (Figure 5g). This observation was confirmed by a greatly reduced accumulation of SCL23:YFP in *shr* mutant roots (Figure 5d,d′), and in agreement with a previous study showing regulation of

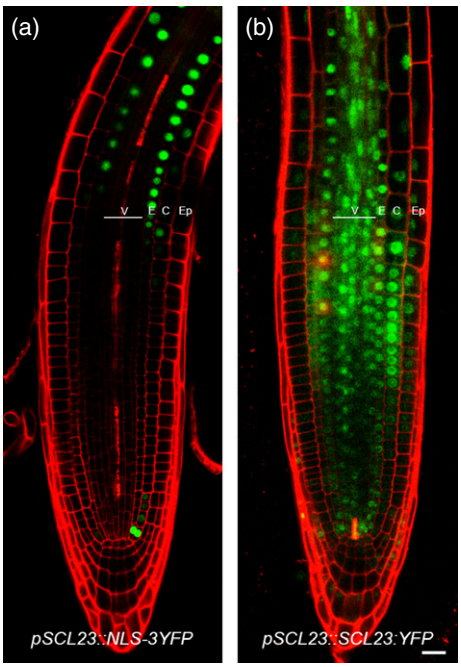

Figure 3. Root expression pattern of SCARECROW-LIKE23 (SCL23). Expression pattern of SCL23 depicted by *pSCL23::NLS-3YFP* (a) and *pSCL23::SCL23:YFP* (b). Scale bar = 20 μm.

SCL23 by SHR in the shoot (Cui *et al.*, 2014). However, in *scr*, both *SCL23* transcript and SCL23 protein levels were increased (Figure 5e,e′,g) suggesting that SCR negatively regulates transcription of *SCL23*. We then assessed the level of SCL23 protein in roots ectopically expressing SCR in the stele under the *pWOL* promoter, and found reduced SCL23 expression in the meristem correlating with high *pWOL:SCR:mRFP* expression (Figure 5f,f′). These results indicate that *SCR* represses *SCL23* transcription in the root meristem. Nevertheless, SCL23 is expressed in the endodermis shootward from the meristem where SCR is also present, indicating that additional factors are involved in its regulation. We then asked whether transcription of *SCR* is altered in the *scl23* mutant. Quantitative RT-PCR analysis of *SCR* mRNA levels did not reveal a significant change of *SCR* transcript levels compared with WT (Figure 5h).

Taken together, our data suggest that SCR negatively regulates transcription of *SCL23* while SCL23 can influence levels of SCR via its control over the accumulation of SHR.

The SCL23 protein moves inward from the ground tissue to the stele and rootward from the elongation zone to the meristem

The bias in *SCL23* transcript and SCL23 protein localization suggests that SCL23 protein can move from the ground tissue into the central stele and from the elongation zone rootward to the meristem. Radial movement of SCL23 has also been suggested before (Rim *et al.*, 2011). To determine the direction of movement of SCL23, we ectopically expressed SCL23:YFP under promoters marking different cell types and tracked its mobility between cell layers. We first monitored SCL23 expression under the *pCO2* promoter, which is expressed predominantly in the cortex (Figure 6a,a′; Heidstra *et al.*, 2004), and found SCL23:YFP signal not only in the cortex but also in the endodermis and pericycle (Figure 6b,b′). Similarly, when SCL23:YFP was driven by the *pEN7* promoter, predominantly expressed in the endodermis (Figure 6c,c′; Heidstra *et al.*, 2004), signal could also be detected spreading into the pericycle from endodermis (Figure 6d,d′). When expressed in the epidermal lineage under the *WEREWOLF* promoter (*pWER*; Figure 6e,e′; Lee and Schiefelbein, 1999), SCL23:YFP kept its nucleocytoplasmic localization but failed to move inwards (Figure 6f,f′). When expressed in the stele under *pWOL* (Figure 6g,g′), SCL23:YFP was restricted to the stele (Figure 6h,h′).

To test its rootward movement, we constructed the SCL23:YFP protein fusion under the promoter of *SODIUM POTASSIUM ROOT DEFECTIVE1* (*pNaKR1*) reported to be active only in phloem companion cells shootward from the root meristem (Tian *et al.*, 2010). Indeed when *pNaKR1::H2B:YFP* and *pNaKR1::JKD:YFP* were introduced in WT roots, signals were only detected in a subset of vascular cell files in the elongation zone (Figure 7a,b). However, *pNaKR1::SCL23:YFP* signal was detectable not only in the *pNaKR1* domain but also in the meristemic stele, indicating that SCL23:YFP has moved rootward (Figure 7c). Additionally, weak signal was also visible in the endodermis, cortex and epidermis of *pNaKR1::SCL23:YFP* roots, predominantly in the transition zone (Figure 7c′). This suggests that SCL23 can also move out of the stele. Interestingly, no longitudinal or radial SHR:YFP spread was detected from the *pNaKR1* domain (Figure 7d; Sena *et al.*, 2004). Together with its aforementioned expression pattern, these data confirm that SCL23 protein moves rootward and preferentially inwards, i.e. from the ground tissue into the stele.

DISCUSSION

In this report, we identified SCL23 as a mobile protein controlling endodermal specification jointly with its binding partner SCR. The SCL23 protein belongs to the GRAS domain protein family, and is the closest homolog to SCR in monocot and dicot plants (Lee *et al.*, 2008). Interestingly, despite being highly homologous to SCR, SCL23 lacks the N-terminal region upstream of the GRAS domain. SCR protein variant that lacks this N-terminal region fails to be restricted to the nucleus (Cui and Benfey, 2009) and acquired the ability to move outwards when expressed in the stele (Gallagher and Benfey, 2009). In addition, when the N-terminal region of SCR was artificially attached to SHR, it promoted nuclear localization of SHR and limited its movement (Gallagher and Benfey, 2009). These data

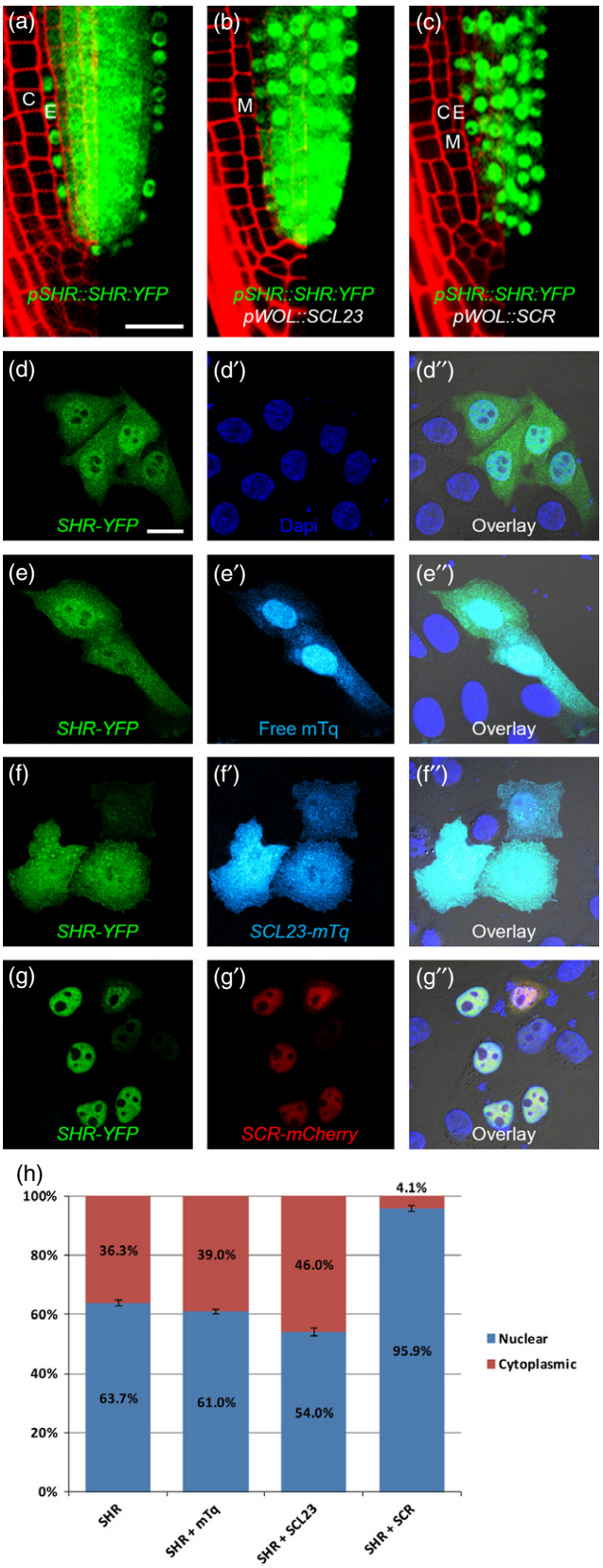

Figure 4. SCARECROW-LIKE23 (SCL23) restricts spreading out of SHOOT-ROOT (SHR) without nuclear retention.
(a)–(c) SHR:YFP exhibits nucleocytoplasmic localization in the stele but nuclear localization in the endodermis (a). *pWOL::SCL23* retards exit of SHR:YFP from the stele, while retaining its nucleocytoplasmic distribution (b). *pWOL::SCR* retards exit of SHR:YFP from the stele by nuclear retention (c). Ectopic expression of both SCR and SCL23 resulted in a ground tissue monolayer. The left parts show the SHR:YFP signal overlaid with cell walls stained with propidium iodide, while the right parts show the SHR:YFP signal only. C, cortex; E, endodermis; M, ground tissue monolayer. (d)–(g″) HeLa cell analysis of SHR-YFP nuclear retention. SHR-YFP exhibits nucleocytoplasmic localization, similar to that in the stele (d–d″). Free mTurquoise (mTq) was used as a negative control (e–e″). SCL23-mTq fails to enrich SHR-YFP into nuclei (f–f″), while SCR-mCherry promotes near-complete nuclear accumulation of SHR-YFP (g–g″). Scale bars = 20 μm. (h) Quantification of HeLa cell analysis in (d)–(g″). Error bars represent standard errors of means.

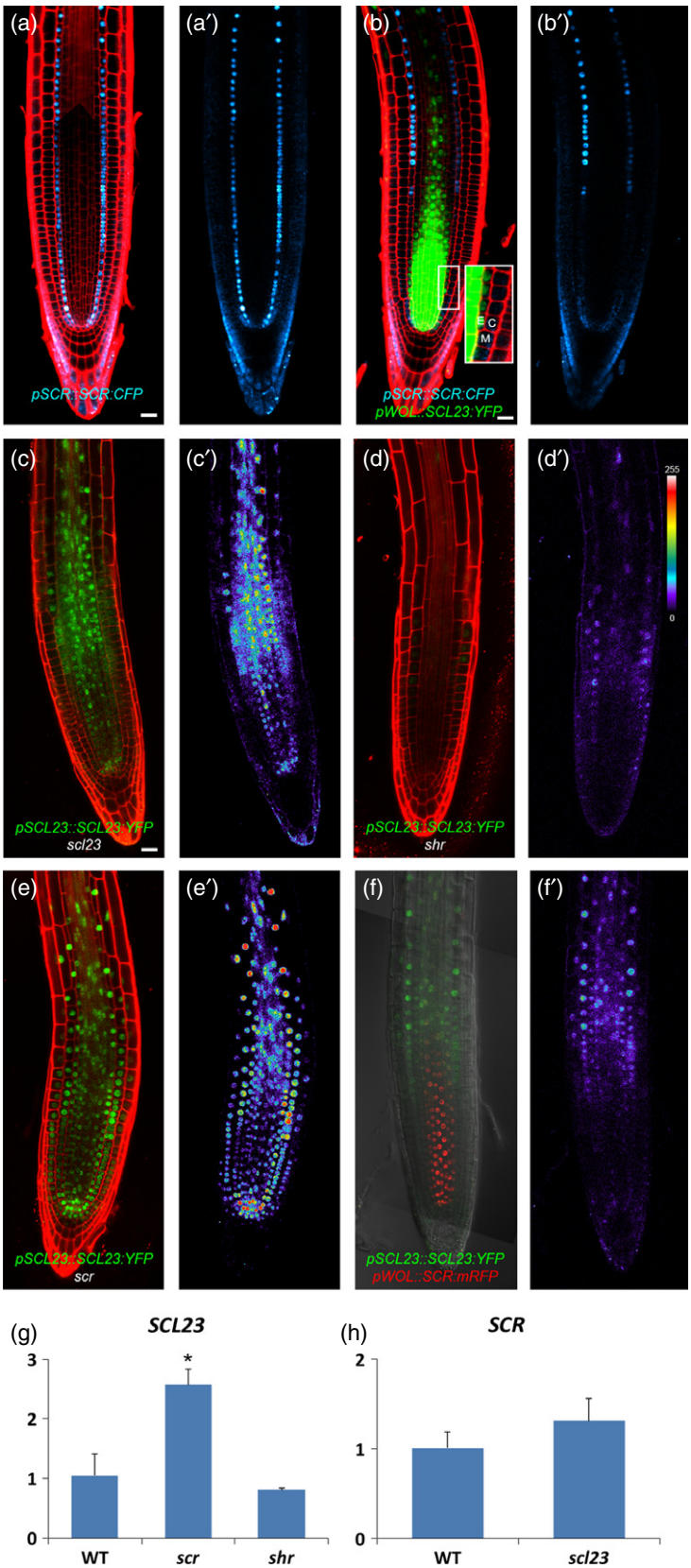

Figure 5. Transcriptional regulation between SCARECROW-LIKE23 (SCL23) and SCARECROW (SCR).

(a)–(b′) pSCR::SCR:CFP expression in wild-type (WT) root (a,a′). Ectopic *pWOL::SCL23:YFP* abolished *pSCR::SCR:CFP* expression in the root meristem, while SCR expression is resumed in the transition zone (b, b′). (a′) and (b′) are signals of the CFP channel from (a) and (b). Note that the cyan signal near the stem cell niche in (b′) is excluded from nuclei, and represents autofluorescence which is also present in (a′).

(c)–(f′) The *pSCL23::SCL23:YFP* level in *scl23* (c, c′), *shr* (d, d′), *scr* (e, e′) and *pWOL::SCR:RFP* lines (f, f′). The SCL23:YFP signal level is depicted in the intensity heatmap in (c′)–(f′). The heatmap pseudocolor scale is as presented (see online version for best detail). Scale bars – 20 μm. (g) *SCL23* mRNA levels in WT, *scr* ($P = 0.03$, asterisk) and *shr* ($P = 0.18$) determined by quantitative (q)RT-PCR. Error bars represent standard deviations. (h) *SCR* mRNA levels in WT and *scl23* determined by qRT-PCR. Error bars represent standard deviations.

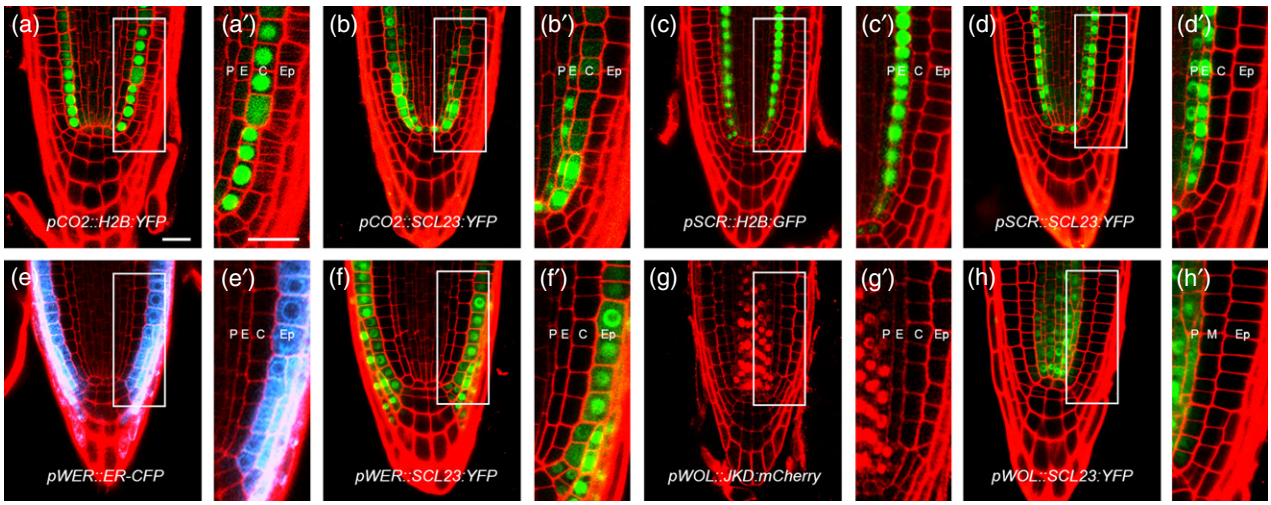

Figure 6. SCARECROW-LIKE23 (SCL23) protein moves inward from the ground tissue to the stele.
(a)–(h′) SCL23 moves from the ground tissue to the stele. *pCO2::H2B:YFP* (a, a′), *pCO2::SCL23:YFP* (b, b′), *pSCR::H2B:GFP* (c, c′), *pSCR::SCL23:YFP* (d, d′), *pWER::ER-CFP* (e, e′), *pWER::SCL23:YFP* (f, f′), *pWOL::JKD:mCherry* (g, g′), *pWOL::SCL23:YFP* (h, h′). (a′)–(h′) Enlarged images of the boxed regions in (a)–(h). P, pericycle; E, endodermis; C, cortex; Ep, epidermis; M, ground tissue monolayer. Scale bars = 20 μm.

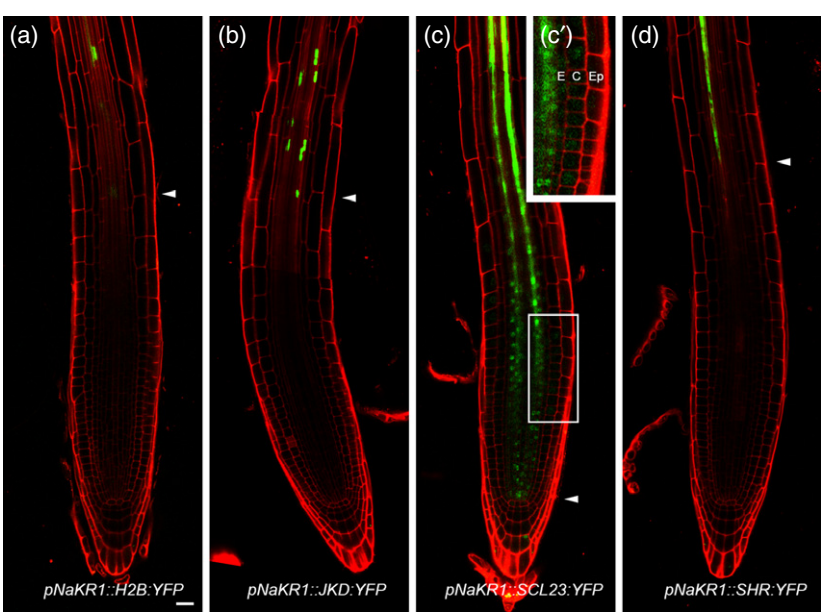

Figure 7. SCARECROW-LIKE23 (SCL23) protein moves rootward from elongation zone to meristem.
(a)–(d) SCL23:YFP moves from the *pNaKR1* domain of mature phloem companion cells (c, c′), while H2B:YFP (a), JKD:YFP (b) or SHR:YFP (d) does not move from this domain. Arrowheads point to the most rootward signal. Brightness and contrast are increased in (c′) to enhance SCL23:YFP visualization outside the stele. Scale bar = 20 μm.

suggest that the difference in localization and mobility between SCR and SCL23 might be conferred by this region. However, SCR lacking the N-terminal domain did not mimic SCL23 localization or acquire the ability for inward movement (Cui and Benfey, 2009), indicating that SCL23 might contain specific motifs that attribute its directional intercellular trafficking.

SCL23 is mainly transcribed in the ground tissue starting shootward from the transition zone, while the protein moves inward to the vasculature and rootward into the meristem. Despite showing a general inward movement from meristemic ground tissue (Figure 6; Rim *et al.*, 2011), SCL23 protein can spread outward to the epidermis as well (Figure 3). This is especially notorious in the transition zone where the level of SCL23 is high, and indicates that movement of SCL23 has zone-specific directional preference, with the meristem favoring movement from the ground tissue to the stele (Figure S2) while the transition zone exhibits bidirectional radial movement. Such a directional pattern also suggests that movement of SCL23 is differentially regulated across the root. Dissecting these root zones and identifying regulators of SCL23 movement will advance our understanding of the control mechanisms of intercellular protein trafficking.

The SCL23 protein contributes to endodermis specification redundantly with SCR and downstream of SHR.

Predominantly localized to the stele in the meristem, SCL23 might act in a non-cell-autonomous manner to specify endodermal fate by promoting the stele-originated signal. Alternatively, SCL23 might function cell-autonomously in the transition zone and rootward, where endodermal SCL23 is more abundant, to mediate endodermis maturation. Still, the single *scl23* mutant did not show any alteration in root pattern when observed under normal growth conditions. Being a member of the large SCR-like family, it is conceivable to that SCL23 is functionally redundant with closely related members and may exhibit gene-specific functions only under specific growth conditions.

Additionally, the double mutant *scr scl23* also mimics the *shr* phenotypes in reducing root length and overall plant size. This suggests that the action of SHR in controlling root and shoot development is mediated by joint action of SCR and SCL23. Isolating SCL23 targets and domain-specific rescue in the roots will provide more insights into the exact function of SCL23. Interestingly, SCL23 is also involved in the establishment of the bundle sheath, a specialized cell layer outside the leaf vasculature or vein, together with SCR and SHR (Cui *et al.*, 2014). The similar molecular determinants for endodermis and bundle sheath confirm that they are analogous cell types (Cui *et al.*, 2014). The SHR protein was also found one cell layer outside the leaf vein where it is transcribed, indicating that SHR's pattern of movement is also conserved in roots and leaves (Gardiner *et al.*, 2011). However, it remains to be tested whether movement of SHR is required for bundle sheath formation. In addition, SCL23 movement has not yet been documented in aboveground tissues, and it will be interesting to examine whether SCL23 is mobile in leaves.

While we have identified SCL23 as a mobile molecule with a distinct directionality of trafficking compared with SHR, it is unclear to what extent this movement is relevant to its function. It remains to be established whether SCL23 trafficking is required for regulation of the movement of SHR, endodermal specification or both. One possibility is that SCL23 might counter the outspread of SHR by binding and back-fluxing it (Figure S2). As SHR is equally distributed after the CEI has divided into the first endodermis and cortex cells (Nakajima *et al.*, 2001), the early ground tissue expression of *SCL23* might function to reduce SHR activity to prevent additional divisions or maintain a delayed division status in the CEI.

In plants, many transcription factors have been found to translocate between cells and exert functions outside their transcriptional domains (Reviewed by Han *et al.*, 2014). Many of these transcription factors, such as LFY and WUSCHEL (WUS), seem to diffuse between cells (Sessions *et al.*, 2000; Yadav *et al.*, 2011), while others, such as TARGET OF MONOPTEROS 7 (TMO7), move in a specific direction and/or with a specific range (Schlereth *et al.*, 2010; Rim *et al.*, 2011). We show that movement of both SHR and SCL23 is directional and partially opposite. The SHR and SCL23 proteins can form complexes with each other and with the immobile SCR to regulate the range of movement of SHR and to specify endodermis. Similarly, the floral homeotic MADS-box proteins DEFICIENS (DEF) and GLOBOSA (GLO) in *Antirrhinum majus* were shown to move within the floral meristem and form protein complexes to specify petal and stamen identities (Schwarz-Sommer *et al.*, 1992; Perbal *et al.*, 1996). It is likely that many more plant developmental processes require the combined activities of mobile transcription factors, and a thorough characterization of these factors is required to understand plant development as a whole.

EXPERIMENTAL PROCEDURES

Yeast two-hybrid screen

A yeast two-hybrid library was constructed from cDNA derived from cDNA 5-day-old *Arabidopsis* roots according to the CloneMiner cDNA Library Construction Kit (Invitrogen, http://www.invitrogen.com/) and transferred into pDEST22 using Gateway technology. This library was amplified once and subsequently plasmid DNA was isolated using the Qiagen HiSpeed Plasmid Midi Kit (http://www.qiagen.com/).

Screening was performed with 5 mM 3AT (3-amino-1,2,4-triazole) to prevent false positive detection due to low autoactivation by the DBD:SCR fusion protein.

Growth condition and plant lines

Growth conditions of *Arabidopsis thaliana* ecotype Columbia-0 (Col-0) are as described by Sabatini *et al.* (1999). The following mutant and transgenic lines used: *scr-3* (Fukaki *et al.*, 1996); *shr-2* (Nakajima *et al.*, 2001); *scl23-2* (Lee *et al.*, 2008); *pCO2::H2B:YFP* and *pSCR::H2B:YFP* (Heidstra *et al.*, 2004); *pWER::ER-CFP* (Willemsen *et al.*, 2008); *pWOL::JKD:mCherry* (Long *et al.*, 2015b). The SHR and SCR fluorescent fusion lines are as described in Long *et al.*, 2015b). Double mutants were generated by crossing.

Constructs for plants and cells

The coding sequence (CDS) of *SCL23* was amplified using primers in Table S1 and subcloned into pDONR221 by Gateway BP reaction (Invitrogen). A position approximately 1.7 kb upstream of the *SCL23* start codon was selected for the *SCL23* promoter (*pSCL23*) and introduced into pGEMteasy1R4. Promoters such as *pNaKR1* (Tian *et al.*, 2010), *pCO2* and *pEN7* were also subcloned into pGEMteasy1R4 vectors. *pWER* and *pWOL* are as described in (Hassan *et al.*, 2010). Plant expression vectors were created by Multisite Gateway LR reactions (Invitrogen).

The CDS of *SCL23* was also subcloned into the HeLa expression vector mTurquoise-N1 (Goedhart *et al.*, 2010). Other HeLa expression vectors are as described in Long *et al.* (2015b).

Bimolecular fluorescence complementation assay

The S*CL23* CDS in pDONR221 was recombined into the pACR233 vector for BiFC analysis. Other BiFC vectors are as described in Welch *et al.* (2007) and Cruz-Ramírez *et al.* (2012).

Arabidopsis thaliana Col-0 mesophyll protoplasts were prepared and transfected according to Yoo *et al.* (2007) with the following adaptations: fourth and fifth leaves from young seedings were incised on the abaxial side and laid on the surface of an enzyme solution for overnight digestion. A 40% PEG-calcium transfection solution was used during transfection. A total of 2×10^5 protoplast cells were used for each transfection. Five micrograms of each BiFC vector were transfected. After transfection, W5 solution was used instead of WI, and transfected protoplasts were cultivated overnight under constant light before observation.

FRET-FLIM

The SCL23 *CDS* in pDONR221 was introduced between the cauliflower mosaic virus *35S* promoter and *SYFP2* by a Multisite Gateway LR reaction (Invitrogen). Constructs used for FRET-FLIM in plants and HeLa cells are described in (Long *et al.*, 2015b).

Living transfected protoplasts were collected in LabTek chambered coverglass (Nunc, http://www.thermoscientific.com) for FLIM according to Goedhart *et al.* (2007). HeLa cells were transfected according to Long *et al.* (2015b) and FLIM was performed as described in Goedhart *et al.* (2010). mTurquoise and SYFP2-fused samples were excited with a 440-nm modulated diode laser (LDH-M-C-440; PicoQuant) or a 514-nm argon laser (Melles-Griot, http://mellesgriot.com/) intensity modulated at a frequency of 75.1 MHz. The light was reflected by a 455DCLP or a 525DCXR dichroic mirror and emission was passed through a D480/40 or a HQ545/30 band-pass emission filter (Chroma Technology, https://www.chroma.com/). Emissions were detected using a radio frequency (RF)-modulated image intensifier (Lambert Instruments II18MD, http://www.lambertinstruments.com/) coupled to a charge-coupled device (CCD) camera (Photometrics HQ, http://www.photometrics.com/). We acquired FLIM stacks of 18 phase images in permutated recording order with an exposure time of 50–1000 ms per image, depending on sample brightness. The FRET efficiency, based on τ_φ or τ_{mod}, was calculated as described in Goedhart *et al.* (2007). More than 60 cells were analyzed for each sample.

Confocal microscopy

Roots were mounted in 10 μM propidium iodide for cell wall visualization. HeLa cells were transfected and fixed as in Long *et al.* (2015b). Confocal microscopy was performed using Leica SP2 and Zeiss LSM710 confocal microscopes as described in Wachsman *et al.* (2011) and Long *et al.* (2015b). The nuclear/cytoplasmic ratio of SHR-YFP was determined by plotting the mean intensities of three regions of interest in the nucleus and cytoplasm of each HeLa cell with background extraction measured by using ImageJ according to Long *et al.* (2015b).

Quantitative RT-PCR

Total RNA was extracted from 7-day-old seedlings (Spectrum Plant Total RNA Kit; Sigma-Aldrich, http://www.sigmaaldrich.com/). The DNase treatment and cDNA synthesis were performed according to the manufacturer's description (ThermoFisher, https://www.thermofisher.com). Quantitative RT-PCR was performed using SYBR Green Mastermix (Applied Biosystems, http://www.appliedbiosystems.com). Results were normalized against ACTIN expression.

Casparian strip visualization

Six-day-old roots were cleared according to Alassimone *et al.* (2010). Cleared roots were mounted in 50% glycerol and Casparian strip autofluorescence was visualized at 520–580 nm by 514-nm laser excitation.

Image processing

For images showing long root regions, overlapping confocal images were stitched together with Adobe Photoshop (http://www.adobe.com/; Figures 3, 5a–f′, 7). All root images were rotated to vertical orientation in Adobe Photoshop, and the resulting empty area was filled with black pixels to generate rectangular panels (Figures 2d–i′, 3, 4a–c, 5a–f′, 6, 7).

ACKNOWLEDGEMENTS

This work was supported by an NWO VIDI grant for IB and YL. YL was further supported by ERC Advanced Grant SysArc and a NWO Spinoza Grant to BS.

SUPPORTING INFORMATION

Additional Supporting Information may be found in the online version of this article.

Figure S1. Förster resonance energy transfer measurement using the fluorescence-lifetime imaging microscopy (FRET-FLIM) analysis between SHORT-ROOT, SCARECROW and SCARECROW-LIKE23 in HeLa cells.

Figure S2. Schematic representation of SHORT-ROOT and SCARECROW-LIKE23 showing directional movement and transcriptional regulation in the meristem.

Table S1. Primers used in this study.

REFERENCES

Alassimone, J., Naseer, S. and Geldner, N. (2010) A developmental framework for endodermal differentiation and polarity. *Proc. Natl Acad. Sci.* **107**, 5214–5219. Available at: [Accessed May 25, 2015].

Benfey, P.N., Linstead, P.J., Roberts, K., Schiefelbein, J.W., Hauser, M.T. and Aeschbacher, R.A. (1993) Root development in *Arabidopsis*: four mutants with dramatically altered root morphogenesis. *Development*, **119**, 57–70.

Birnbaum, K., Jung, J.W., Wang, J.Y., Lambert, G.M., Hirst, J.A., Galbraith, D.W. and Benfey, P.N. (2005) Cell type-specific expression profiling in plants via cell sorting of protoplasts from fluorescent reporter lines. *Nat. Methods*, **2**, 615–619.

Bonke, M., Thitamadee, S., Mähönen, A.P., Hauser, M.-T. and Helariutta, Y. (2003) APL regulates vascular tissue identity in *Arabidopsis*. *Nature*, **426**, 181–186.

Brady, S.M., Orlando, D.A., Lee, J.-Y., Wang, J.Y., Koch, J., Dinneny, J.R., Mace, D., Ohler, U. and Benfey, P.N. (2007) A high-resolution root spatiotemporal map reveals dominant expression patterns. *Science*, **318**, 801–806.

Cruz-Ramírez, A., Díaz-Triviño, S., Blilou, I. *et al.* (2012) A bistable circuit involving SCARECROW-RETINOBLASTOMA integrates cues to inform asymmetric stem cell division. *Cell*, **150**, 1002–1015.

Cruz-Ramírez, A., Díaz-Triviño, S., Wachsman, G. *et al.* (2013) A SCARECROW-RETINOBLASTOMA protein network controls protective quiescence in the *Arabidopsis* root stem cell organizer. *PLoS Biol.* **11**, e1001724.

Cui, H. and Benfey, P.N. (2009) Interplay between SCARECROW, GA and LIKE HETEROCHROMATIN PROTEIN 1 in ground tissue patterning in the *Arabidopsis* root. *Plant J.* **58**, 1016–1027.

Cui, H., Levesque, M.P., Vernoux, T. *et al.* (2007) An evolutionarily conserved mechanism delimiting SHR movement defines a single layer of endodermis in plants. *Science*, **316**, 421–425.

Cui, H., Kong, D., Liu, X. and Hao, Y. (2014) SCARECROW, SCR-LIKE 23 and SHORT-ROOT control bundle sheath cell fate and function in *Arabidopsis thaliana*. *Plant J.* **78**, 319–327.

Dolan, L. (2006) Positional information and mobile transcriptional regulators determine cell pattern in the *Arabidopsis* root epidermis. *J. Exp. Bot.* **57**, 51–54.

Fukaki, H., Fujisawa, H. and Tasaka, M. (1996) SGR1, SGR2, SGR3: novel genetic loci involved in shoot gravitropism in *Arabidopsis thaliana*. *Plant Physiol.* **110**, 945–955.

Gallagher, K.L. and Benfey, P.N. (2009) Both the conserved GRAS domain and nuclear localization are required for SHORT-ROOT movement. *Plant J.* **57**, 785–797.

Gallagher, K.L., Sozzani, R. and Lee, C.-M. (2014) Intercellular protein movement: deciphering the language of development. *Annu. Rev. Cell Dev. Biol.* **30**, 207–233.

Gardiner, J., Donner, T.J. and Scarpella, E. (2011) Simultaneous activation of SHR and ATHB8 expression defines switch to preprocambial cell state in *Arabidopsis* leaf development. *Dev. Dyn.* **240**, 261–270.

Goedhart, J., Vermeer, J.E.M., Adjobo-Hermans, M.J.W., van Weeren, L. and Gadella, T.W.J. Jr (2007) Sensitive detection of p65 homodimers using red-shifted and fluorescent protein-based FRET couples. *PLoS One*, **2**, e1011. Available at: [Accessed March 27, 2014].

Goedhart, J., van Weeren, L., Hink, M.A., Vischer, N.O.E., Jalink, K. and Gadella, T.W.J. (2010) Bright cyan fluorescent protein variants identified by fluorescence lifetime screening. *Nat. Methods*, **7**, 137–139. Available at: [Accessed March 25, 2014].

Han, X., Kumar, D., Chen, H., Wu, S. and Kim, J.-Y. (2014) Transcription factor-mediated cell-to-cell signalling in plants. *J. Exp. Bot.* **65**, 1737–1749.

Hassan, H., Scheres, B. and Blilou, I. (2010) JACKDAW controls epidermal patterning in the *Arabidopsis* root meristem through a non-cell-autonomous mechanism. *Development*, **137**, 1523–1529.

Heidstra, R., Welch, D. and Scheres, B. (2004) Mosaic analyses using marked activation and deletion clones dissect *Arabidopsis* SCARECROW action in asymmetric cell division. *Genes Dev.* **18**, 1964–1969.

Helariutta, Y., Fukaki, H., Wysocka-Diller, J., Nakajima, K., Jung, J., Sena, G., Hauser, M.T. and Benfey, P.N. (2000) The SHORT-ROOT gene controls radial patterning of the *Arabidopsis* root through radial signaling. *Cell*, **101**, 555–567.

Kerstetter, R.A., Laudencia-Chingcuanco, D., Smith, L.G. and Hake, S. (1997) Loss-of-function mutations in the maize homeobox gene, knotted1, are defective in shoot meristem maintenance. *Development*, **124**, 3045–3054.

Kim, J.Y., Yuan, Z., Cilia, M., Khalfan-Jagani, Z. and Jackson, D. (2002) Intercellular trafficking of a KNOTTED1 green fluorescent protein fusion in the leaf and shoot meristem of *Arabidopsis*. *Proc. Natl Acad. Sci. USA*, **99**, 4103–4108.

Kim, J.-Y., Yuan, Z. and Jackson, D. (2003) Developmental regulation and significance of KNOX protein trafficking in *Arabidopsis*. *Development*, **130**, 4351–4362.

Kim, J.-Y., Rim, Y., Wang, J. and Jackson, D. (2005) A novel cell-to-cell trafficking assay indicates that the KNOX homeodomain is necessary and sufficient for intercellular protein and mRNA trafficking. *Genes Dev.* **19**, 788–793.

Koizumi, K., Hayashi, T., Wu, S. and Gallagher, K.L. (2012) The SHORT-ROOT protein acts as a mobile, dose-dependent signal in patterning the ground tissue. *Proc. Natl Acad. Sci. USA*, **109**, 13010–13015.

Kragler, F., Monzer, J., Xoconostle-Cázares, B. and Lucas, W.J. (2000) Peptide antagonists of the plasmodesmal macromolecular trafficking pathway. *EMBO J.* **19**, 2856–2868.

Di Laurenzio, L., Wysocka-Diller, J., Malamy, J.E., Pysh, L., Helariutta, Y., Freshour, G., Hahn, M.G., Feldmann, K.A. and Benfey, P.N. (1996) The SCARECROW gene regulates an asymmetric cell division that is essential for generating the radial organization of the *Arabidopsis* root. *Cell*, **86**, 423–433.

Lee, M.M. and Schiefelbein, J. (1999) WEREWOLF, a MYB-related protein in *Arabidopsis*, is a position-dependent regulator of epidermal cell patterning. *Cell*, **99**, 473–483.

Lee, M.-H., Kim, B., Song, S.-K. *et al.* (2008) Large-scale analysis of the GRAS gene family in *Arabidopsis thaliana*. *Plant Mol. Biol.* **67**, 659–670.

Levesque, M.P., Vernoux, T., Busch, W. *et al.* (2006) Whole-genome analysis of the SHORT-ROOT developmental pathway in *Arabidopsis*. *PLoS Biol.* **4**, e143.

Lohmann, J.U., Hong, R.L., Hobe, M., Busch, M.A., Parcy, F., Simon, R. and Weigel, D. (2001) A molecular link between stem cell regulation and floral patterning in *Arabidopsis*. *Cell*, **105**, 793–803.

Long, J.A., Moan, E.I., Medford, J.I. and Barton, M.K. (1996) A member of the KNOTTED class of homeodomain proteins encoded by the STM gene of *Arabidopsis*. *Nature*, **379**, 66–69.

Long, Y., Scheres, B. and Blilou, I. (2015a) The logic of communication: roles for mobile transcription factors in plants. *J. Exp. Bot.* **66**, 1133–1144.

Long, Y., Smet, W., Cruz-Ramírez, A. *et al.* (2015b) *Arabidopsis* BIRD zinc finger proteins jointly stabilize tissue boundaries by confining the cell fate regulator SHORT-ROOT and contributing to fate specification. *Plant Cell*, **27**, 1185–1199.

Lucas, W.J., Bouché-Pillon, S., Jackson, D.P., Nguyen, L., Baker, L., Ding, B. and Hake, S. (1995) Selective trafficking of KNOTTED1 homeodomain protein and its mRNA through plasmodesmata. *Science*, **270**, 1980–1983.

Mähönen, A.P., ten Tusscher, K., Siligato, R. *et al.* (2014) PLETHORA gradient formation mechanism separates auxin responses. *Nature*, **515**, 125–129.

Nakajima, K., Sena, G., Nawy, T. and Benfey, P.N. (2001) Intercellular movement of the putative transcription factor SHR in root patterning. *Nature*, **413**, 307–311.

Perbal, M.C., Haughn, G., Saedler, H. and Schwarz-Sommer, Z. (1996) Non-cell-autonomous function of the Antirrhinum floral homeotic proteins DEFICIENS and GLOBOSA is exerted by their polar cell-to-cell trafficking. *Development*, **122**, 3433–3441.

Reiser, L., Sánchez-Baracaldo, P. and Hake, S. (2000) Knots in the family tree: evolutionary relationships and functions of knox homeobox genes. *Plant Mol. Biol.* **42**, 151–166.

Rim, Y., Jung, J., Chu, H., Cho, W.K., Kim, S., Hong, J.C., Jackson, D., Datla, R. and Kim, J. (2009) A non-cell-autonomous mechanism for the control of plant architecture and epidermal differentiation involves intercellular trafficking of BREVIPEDICELLUS protein. *Funct. Plant Biol.* **36**, 280–289. Available at: [Accessed August 29, 2014].

Rim, Y., Huang, L., Chu, H. *et al.* (2011) Analysis of *Arabidopsis* transcription factor families revealed extensive capacity for cell-to-cell movement as well as discrete trafficking patterns. *Mol. Cells*, **32**, 519–526.

Sabatini, S., Beis, D., Wolkenfelt, H. *et al.* (1999) An auxin-dependent distal organizer of pattern and polarity in the *Arabidopsis* root. *Cell*, **99**, 463–472.

Sabatini, S., Heidstra, R., Wildwater, M. and Scheres, B. (2003) SCARECROW is involved in positioning the stem cell niche in the *Arabidopsis* root meristem. *Genes Dev.* **17**, 354–358. Available at: [Accessed May 19, 2014].

Scheres, B. (2001) Plant cell identity. The role of position and lineage. *Plant Physiol.* **125**, 112–114.

Schlereth, A., Möller, B., Liu, W., Kientz, M., Flipse, J., Rademacher, E.H., Schmid, M., Jürgens, G. and Weijers, D. (2010) MONOPTEROS controls embryonic root initiation by regulating a mobile transcription factor. *Nature*, **464**, 913–916.

Schneeberger, R.G., Becraft, P.W., Hake, S. and Freeling, M. (1995) Ectopic expression of the knox homeo box gene rough sheath1 alters cell fate in the maize leaf. *Genes Dev.* **9**, 2292–2304.

Schwarz-Sommer, Z., Hue, I., Huijser, P., Flor, P.J., Hansen, R., Tetens, F., Lönnig, W.E., Saedler, H. and Sommer, H. (1992) Characterization of the Antirrhinum floral homeotic MADS-box gene deficiens: evidence for DNA binding and autoregulation of its persistent expression throughout flower development. *EMBO J.* **11**, 251–263.

Sena, G., Jung, J.W. and Benfey, P.N. (2004) A broad competence to respond to SHORT ROOT revealed by tissue-specific ectopic expression. *Development*, **131**, 2817–2826.

Sessions, A., Yanofsky, M.F. and Weigel, D. (2000) Cell-cell signaling and movement by the floral transcription factors LEAFY and APETALA1. *Science*, **289**, 779–782.

Sparks, E., Wachsman, G. and Benfey, P.N. (2013) Spatiotemporal signalling in plant development. *Nat. Rev. Genet.* **14**, 631–644.

Tian, H., Baxter, I.R., Lahner, B., Reinders, A., Salt, D.E. and Ward, J.M. (2010) *Arabidopsis* NPCC6/NaKR1 is a phloem mobile metal binding protein necessary for phloem function and root meristem maintenance. *Plant Cell*, **22**, 3963–3979.

Vollbrecht, E., Reiser, L. and Hake, S. (2000) Shoot meristem size is dependent on inbred background and presence of the maize homeobox gene, knotted1. *Development*, **127**, 3161–3172.

Wachsman, G., Heidstra, R. and Scheres, B. (2011) Distinct cell-autonomous functions of RETINOBLASTOMA-RELATED in *Arabidopsis* stem cells revealed by the Brother of Brainbow clonal analysis system. *Plant Cell*, **23**, 2581–2591. Available at: [Accessed May 25, 2015].

Weigel, D., Alvarez, J., Smyth, D.R., Yanofsky, M.F. and Meyerowitz, E.M. (1992) LEAFY controls floral meristem identity in *Arabidopsis*. *Cell*, **69**, 843–859.

Welch, D., Hassan, H., Blilou, I., Immink, R., Heidstra, R. and Scheres, B. (2007) *Arabidopsis* JACKDAW and MAGPIE zinc finger proteins delimit asymmetric cell division and stabilize tissue boundaries by restricting SHORT-ROOT action. *Genes Dev.* **21**, 2196–2204.

Willemsen, V., Bauch, M., Bennett, T., Campilho, A., Wolkenfelt, H., Xu, J., Haseloff, J. and Scheres, B. (2008) The NAC domain transcription factors FEZ and SOMBRERO control the orientation of cell division plane in *Arabidopsis* root stem cells. *Dev. Cell*, **15**, 913–922.

Wu, X., Dinneny, J.R., Crawford, K.M., Rhee, Y., Citovsky, V., Zambryski, P.C. and Weigel, D. (2003) Modes of intercellular transcription factor movement in the *Arabidopsis* apex. *Development*, **130**, 3735–3745.

Yadav, R.K., Perales, M., Gruel, J., Girke, T., Jönsson, H. and Reddy, G.V. (2011) WUSCHEL protein movement mediates stem cell homeostasis in the *Arabidopsis* shoot apex. *Genes Dev.* **25**, 2025–2030.

Yoo, S.-D., Cho, Y.-H. and Sheen, J. (2007) *Arabidopsis* mesophyll protoplasts: a versatile cell system for transient gene expression analysis. *Nat. Protoc.* **2**, 1565–1572.